Vanilloids induce oral cancer apoptosis independent of TRPV1

Cara B. Gonzales [a,b,*], Nameer B. Kirma [a,c], Jorge J. De La Chapa [b], Richard Chen [b], Michael A. Henry [d], Songjiang Luo [b], Kenneth M. Hargreaves [d,e]

[a] Cancer Therapy and Research Center, UTHSCSA, San Antonio, TX 78229, USA
[b] Comprehensive Dentistry, UTHSCSA Dental School, San Antonio, TX 78229, USA
[c] Molecular Medicine, UTHSCSA, San Antonio, TX 78229, USA
[d] Endodontics, UTHSCSA Dental School, San Antonio, TX 78229, USA
[e] Pharmacology, UTHSCSA Dental School, San Antonio, TX 78229, USA

ARTICLE INFO

SUMMARY

Objective: To investigate the mechanisms of vanilloid cytotoxicity and anti-tumor effects in oral squamous cell carcinoma (OSCC).
Materials and methods: Immunohistochemistry and qPCR analyses demonstrated expression of the TRP vanilloid type 1 (TRPV1) receptor in OSCC. Using cell proliferation assays, calcium imaging, and three mouse xenograft models, prototypical vanilloid agonist (capsaicin) and antagonist (capsazepine) were evaluated for cytotoxic and anti-tumor effects in OSCC.
Results: OSCC cell lines treated with capsaicin displayed significantly reduced cell viability. Pre-treatment with capsazepine failed to reverse these effects. Moreover, capsazepine alone was significantly cytotoxic to tumor cells, suggesting the mechanism-of-action is independent of TRPV1 activation. This was further confirmed by calcium imaging indicating that TRPV1 channels are not functional in the cell lines tested. We then examined whether the observed vanilloid cytotoxicity was due to the generation of reactive oxygen species (ROS) and subsequent apoptosis. Induction of ROS was confirmed by flow cytometry and reversed by co-treatment with the antioxidant N-acetyl-cysteine (NAC). NAC also significantly reversed vanilloid cytotoxicity in cell proliferation assays. Dose-dependent induction of apoptosis with capsazepine treatment was demonstrated by FACS analyses and c-PARP expression in treated cells. Our *in vivo* xenograft studies showed that intra-tumoral injections of capsazepine exhibited high effectiveness in suppressing tumor growth with no identifiable toxicities.
Conclusions: These findings confirm TRPV1 channel expression in OSCC. However anti-tumor effects of vanilloids are independent of TRPV1 activation and are most likely due to ROS induction and subsequent apoptosis. Importantly, these studies demonstrate capsazepine is a potential therapeutic candidate for OSCC.

Introduction

Oral squamous cell carcinoma (OSCC) is the 8th most common cancer in the United States with 40,000 new cases and 7,850 deaths reported annually [1]. While the overall survival for early disease (stages 1 and 2) has improved, the death rate has not changed in nearly 40 years [1]. This is due primarily to late-stage disease (stages 3 and 4) that infiltrates adjacent lymph nodes and impinges upon critical structures thereby complicating disease management. Sadly, 60% of OSCC patients have late-stage disease at their initial diagnosis and their five-year survival rate is as low as 30% [1]. Hence there is a great need to develop new therapies aimed at eliminating this insidious disease.

Transient receptor potential (TRP) channels are expressed primarily on pain sensing neurons (nociceptors) and play a major role in transducing sensory stimuli related to pain, temperature, and chemical mediators [2]. TRP channels are predominantly gated by soluble ligands or physical stimuli and act as non-selective cation channels allowing passage of Na^+, Mg^{2+}, and especially Ca^{2+} into cells [2–4]. While TRP channels are characterized extensively in neurons, comparatively little is known about their expression and function in non-neuronal tissues and malignant transformation. Changes in expression of TRP channel subtypes are reported

in multiple tumor types and are deemed potential therapeutic targets for treating cancers [5–22]. It is hypothesized that tumor treatment with TRP channel agonists, specific to their subtype, would result in a large calcium influx thereby inducing apoptosis [5].

Of interest, the vanilloid subtype 1 channel, TRPV1, shows increased expression in prostate, colon and pancreatic cancers with decreased expression in bladder cancer [14–17]. In neurons, TRPV1 responds to noxious stimuli including capsaicin, heat, and low pH [3,4,23]. Both capsaicin and capsazepine are structurally classified as vanilloids as they exert their effects on the TRPV1 channel [24]. Capsaicin, the pungent ingredient in red hot chili peppers, is the natural TRPV1 agonist [3]. Capsazepine is a synthetic TRPV1 antagonist that competitively binds to the channel preventing cation influx and response to noxious stimuli [25].

Previous studies evaluating the effects of vanilloids on cancer cells demonstrate cytotoxicity of capsaicin [5,26,27]. However capsazepine consistently and unexpectedly failed to reverse these effects. Moreover, pre-treatment with TRPV1 antagonists had additive cytotoxic effects and in some studies capsazepine alone was equally if not more cytotoxic than capsaicin [17,26,27]. Some investigators propose that additional members of the TRP channel superfamily may mediate these responses by forming heterogeneous complexes that are activated by capsaicin but not inhibited by capsazepine [27]. Conversely, we hypothesize that vanilloid cytotoxicity on cancer cells results from novel mechanisms that are independent of TRPV1 activation. In the present study we report anti-tumor efficacy of vanilloids via ROS generation and subsequent apoptosis in OSCC cell lines and xenografts.

Materials and methods

Human OSCC Cell Lines

OSCC cell lines, SCC4, SCC25, and HSC3 were derived from human primary tongue OSCC. SCC4 and SCC25 cells were obtained from ATCC (Rockville, MD). HSC3 cells were kindly provided by Dr. Brian Schmidt (NYU) [28]. Cells were maintained in DMEM (Gibco, Carlsbad, CA) containing 10% FBS at 37 °C in 5% CO_2. Immortalized keratinocytes (OKF6-TERT2; Harvard Medical School Cell Culture Core Collection, Cambridge, MA) were used as control epithelial cells.

Immunohistochemical staining

Formalin fixed paraffin-embedded (FFPE) specimens of OSCC and normal oral mucosa ($n = 3$ per group) were obtained from the STRL Core Pathology Laboratory, UTHSCSA. Specimens were deparaffinized, rehydrated, and blocked with 3% normal goat serum. Immunohistochemistry was performed using the Vectastain Elite ABC Kit (Vector Laboratories, Burlingame, CA) according to manufacturer's protocol and TRPV1 (1:100) primary antibody (VR1-748; Affinity BioReagents, Golden, CO). Substrate interactions were visualized with DAB (Vector Laboratories, Burlingame, CA). Negative controls were incubated in pre-immune serum alone.

Reagents

Capsaicin and capsazepine were obtained from Sigma–Aldrich (St. Louis, MO). Stock solutions of capsaicin (50 mg/ml) and capsazepine (5 mg/ml) in 100% EtOH were used *in vitro*. Animal studies used capsazepine stock diluted 20 μg/μl in 100% DMSO.

In vitro capsaicin and capsazepine treatments

OSCC cells (2×10^4) were subcultured into 96-well culture plates for 12 h at 37 °C. Cells were washed with PBS and treated with 150 μM capsaicin and/or with 30 μM capsazepine for 24 h.

Cell viability assays

Cytotoxicity was assessed using the Cell Titer 96® Aqueous Non-Radioactive Cell Proliferation Assay (Promega, Madison, WI) according to manufacturer's protocol. Absorbance values of test groups were normalized against controls ($n = 4$).

Quantitative PCR (qPCR)

Total RNA was isolated using TriReagent (Life Technologies, Hercules, CA) according to the manufacturer's protocol. cDNA synthesis from 500 ng RNA using random primers and Taqman® Reverse Transcription Reagents (Life Technologies, Hercules, CA) was performed according to manufacturer's protocol. QPCR was performed, in triplicate, using Taqman® Gene Expression Assays (Life Technologies, Hercules, CA) for TRPV1 and the housekeeping gene cyclophilin A according to the manufacturer's protocol. Relative changes in TRPV1 mRNA expression were determined using the $2^{-\Delta\Delta C_T}$ method [29].

Immunocytochemistry

OSCC cells were cultured on coverslips (1×10^5), fixed with 4% paraformaldehyde and stained as previously described [30] with Vanilloid Receptor 1 antibody (PA1-748, Thermo Scientific, Rockford, IL), Alexa-Fluor secondary antibody (Molecular Probes, Eugene, OR,) and TO-PRO-3 iodide (TOPRO; Invitrogen, Carlsbad, CA) as a nuclear stain. Images were acquired with a Nikon D-Eclipse microscope and a C1si laser scanning confocal imaging system with a 20×/0.75N objective lens and processed for illustration purposes with Corel DRAW X6 (Corel Corporation, Ottawa, Canada).

Calcium imaging

Calcium imaging was performed using the Fluo-4 Direct Calcium Assay Kit (Life Technologies, Hercules, CA) according to manufacturer's protocol. Cells were incubated with 3 μm Fluo-4 at RT for 30 min then treated with capsaicin alone (20 μM or 150 μM) or pre-treated with capsazepine (10 μM or 30 μM) followed by respective capsaicin treatments; $n = 3$ per group. As a positive control, cells were treated with 3 μM ionomycin, a non-selective cation channel activator. Images were acquired on Sweptfield confocal with a Nikon Ti inverted microscope and a 40× oil immersion/NA1.30 objective for 10 min recordings. Loading and imaging were carried out in recording media (12.78 g/liter DMEM, 5% FBS, 25 μM HEPES, pH 7.2, no phenol red) at 37 °C. Images were analyzed with ImageJ software. Background corrected fluorescence was normalized prior to treatments. Photo-bleaching effect was corrected against vehicle only images collected at the exact settings and focus maintained by the system's Perfect Focus Device.

Flow cytometry

OSCC cell lines were cultured to 50% confluency and treated with 0 μm, 30 μM, 60 μM, and 90 μM capsazepine for 24 h. Cells were harvested, fixed in 70% EtOH, treated with RNase A, and stained with propidium iodide. FACS analysis of DNA profiles in terms of sub-G1, G1, S+G2/M phase of cell cycle was performed.

Immunoblotting

OSCC cell lines treated with vehicle, 30 μM, or 60 μM capsazepine for 24 h were harvested and lysed in 1% Triton-PBS. Cell

lysates (100units/A280) were used for protein electrophoresis in 10% SDS–PAGE. SDS–PAGE separated proteins were transferred to PVDF membrane and the membrane blocked in 5% milk. Anti-cPARP rabbit polyclonal antibody (Cell Signaling, #5625S, Danvers, MA) and anti-β-actin mouse monoclonal antibody (Sigma–Aldrich, #A1978, St. Louis, MO) were diluted 1:1250 in a total of 5 ml diluent (1% milk in PBS-0.1% Tw-20) and incubated overnight at 4 °C. The membrane was washed 3× with PBS-Tw-20, incubated with ECL Plus detection solution (GE Healthcare, South San Francisco, CA) for 1 min and signal detected by exposure to radiograph film for 30 s. Protein lysates from HeLa cells treated with 1 uM paclitaxel for 24 h were used as positive control [31].

Reactive oxygen species (ROS) assays

ROS levels in OSCC cell lines were examined by flow cytometry using 2,7-dichlorodihydrofluorescein diacetate (DCF-DA; Sigma–Aldrich, St. Louis, MO). Cells (3×10^5) were plated in 12-well plates and incubated for 30 min with DCF-DA at 37 °C then treated with 30 μM capsazepine using phenol free media with and without 10 mM NAC. Treated cells were incubated for 1 h at 37 °C, harvested, washed twice, and analyzed by FACS.

Animals

All studies were approved by the UTHSCSA Institutional Animal Care and Use Committee. Six week-old female athymic nude mice (Harlan, Indianapolis, IN) were used in a laminar air-flow cabinet under pathogen-free conditions. They were provided with a 12 h light/dark schedule at controlled temperature and humidity with food and water ad libitum. Mice were acclimated for one week prior to study initiation.

OSCC mouse xenograft models

Mice were injected subcutaneously in the right flank with 2×10^6 HSC3, SCC4, or SCC25 cells in 0.1 ml of sterile PBS. Four weeks post-inoculation, tumors grew to an average volume of
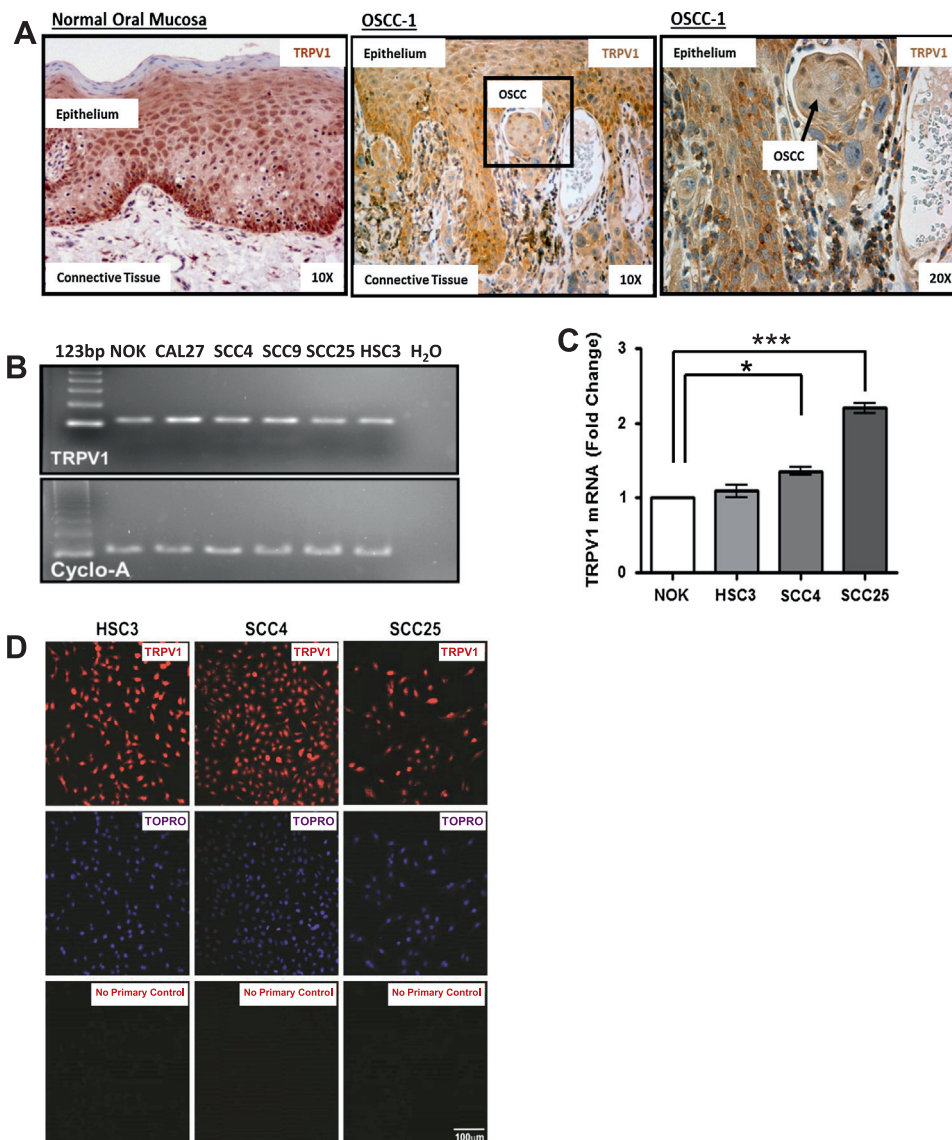

Figure 1. TRPV1 expression in OSCC and normal oral epithelium. *Panel A:* representative photomicrograph of immunohistochemical staining for TRPV1 in normal oral mucosa and OSCC (4X). Epithelium (E), connective tissue (C), OSCC-1 outlined by box. *Panel B:* RT-PCR amplification of TRPV1 mRNA in OSCC cell lines and normal oral keratinocytes (NOK). *Panel C:* QPCR analysis of TRPV1 mRNA expression in OSCC cell lines relative to normal oral keratinocytes (NOK) ($n = 3$); $^*p < 0.05$, $^{***}p < 0.001$. *Panel D:* confocal microscopy shows TRPV1 expression in OSCC cell lines. TRPV1-red, TOPRO DNA staining-blue, no primary antibody control.

110 mm³. Mice were stratified into two experimental groups (n = 5 per group), which received the following treatments as intra-tumoral injections: group A, vehicle control; group B, capsazepine treatment. Treatments were repeated every other day for a total of 12 days (HSC3), 18 days (SCC4), or 16 days (SCC25).

In vivo efficacy analysis of capsazepine in OSCC xenograft models

Capsazepine stock solution (20 µg/µl, 100% DMSO) was diluted to 5% DMSO in sterile saline generating a final concentration of 1 µg/µl. HSC3 and SCC4 xenografts were injected intra-tumorally with 40 µg every other day, while SCC25 were injected intra-tumorally with 20 µg due to reduced size and increased density of SCC25 xenografts. Control xenografts were injected intra-tumorally with vehicle control (5% DMSO). Mice were monitored daily for tumor growth (using digital calipers), cachexia, and weight loss. Body temperature was monitored for 24 h following treatments. Tumor volumes were calculated by the elliptical formula: $1/2(\text{Length} \times \text{Width}^2)$ [32]. At experimental conclusion, blood was collected, and serum stored (-80 °C) for biochemical serum analysis performed by the Mouse Metabolic Phenotyping Center (Yale School of Medicine, New Haven, CT). Tumors were fixed and processed for histological analysis. Hematoxylin and eosin (H&E) staining and terminal deoxynucleotidyl transferase dUTP nick end labeling (TUNEL) to detect apoptotic figures were performed by the UTHSCSA Cancer Therapy and Research Center (CTRC) core pathology laboratory.

Statistical analysis

Statistical analysis was performed using GraphPad Prism4 (San Diego, California). Experiments were performed in triplicate and results are represented as means ± SD except when indicated. QPCR of TRPV1 expression was analyzed using one-way analysis of variance (ANOVA) with Tukey's post hoc test (n = 3). Cytotoxicity assays of cell viability were analyzed by one-way ANOVA and Bonferroni's post hoc test (n = 3). Calcium imaging of OSCC cell lines were analyzed by two-way ANOVA with Bonferroni's post hoc test (n = 3). Statistical analyses of tumor growth were made using analysis of variance with repeated measures with Bonferroni's post hoc test (n = 5). Student's *t*-test was used to evaluate TUNEL staining of apoptotic figures (n = 3; six fields per section) in treated vs. control xenografts. A p value less than 0.05 was considered statistically significant.

Results

TRPV1 channels are differentially expressed in OSCC

Immunohistochemical analysis confirmed the presence of TRPV1 protein in all layers of normal oral epithelium and in OSCC tumors including expression in cells invading deeper connective tissues (Fig. 1A). Analysis of TRPV1 expression in OSCC cell lines and normal oral keratinocytes (NOK) was evaluated using RT-PCR, qPCR and immunofluorescence. Differential expression of TRPV1 mRNA was seen in OSCC cell lines (Fig. 1B) with HSC3 cells expressing relatively equal levels of TRPV1 mRNA compared to NOK, however both SCC4 and SCC25 cells had increased relative expression (~40% and 200% respectively) (Fig. 1C). Immunofluorescence confirmed TRPV1 protein in HSC3, SCC4, and SCC25 cells (Fig. 1D).

Both capsaicin and capsazepine are cytotoxic to OSCC in vitro

Concentration response curves (data not shown) followed by cytotoxicity assays, revealed that capsaicin is cytotoxic to all OSCC

cell lines at high concentrations (150 µM) regardless of differential TRPV1 expression (Fig. 2A). These findings are consistent with previous reports of capsaicin cytotoxicity in other, non-oral cancer cell lines [26,27]. Pre-treatment of cells with capsazepine (30 µM) followed by capsaicin (150 µM) failed to reverse capsaicin cytotoxicity, and instead this combined treatment resulted in significant additive effects with approximately 80% reduction in cell viability (Fig. 2A). This implies that vanilloid cytotoxicity may be due to mechanisms other than TRPV1 activation. Additionally, treatment with equal concentrations of capsaicin (30 µM) vs. capsazepine (30 µM) revealed that capsazepine is significantly cytotoxic to all OSCC cell lines at this lower dose whereas capsaicin was not (Fig. 2A). Treatment of immortalized keratinocytes (OKF6-TERT2) demonstrated that these cells may respond to vanilloids via a TRPV1-mechanism since capsaicin evokes cytotoxicity that is blocked by pre-treatment with capsazepine (30 µM) (Fig. 2B). Furthermore, capsazepine alone demonstrated no toxicity to OKF6-TERT2 cells. These findings make capsazepine an attractive therapeutic compound because, unlike capsaicin, it demonstrates no cytotoxic effects on non-malignant cells *in vitro* [33,34].

TRPV1 channels are not functional in OSCC cell lines

Although TRPV1 channels are present in these cell lines, calcium imaging showed that all OSCC cell lines failed to respond to capsaicin activation at non-cytotoxic concentrations (20 µM) indicating
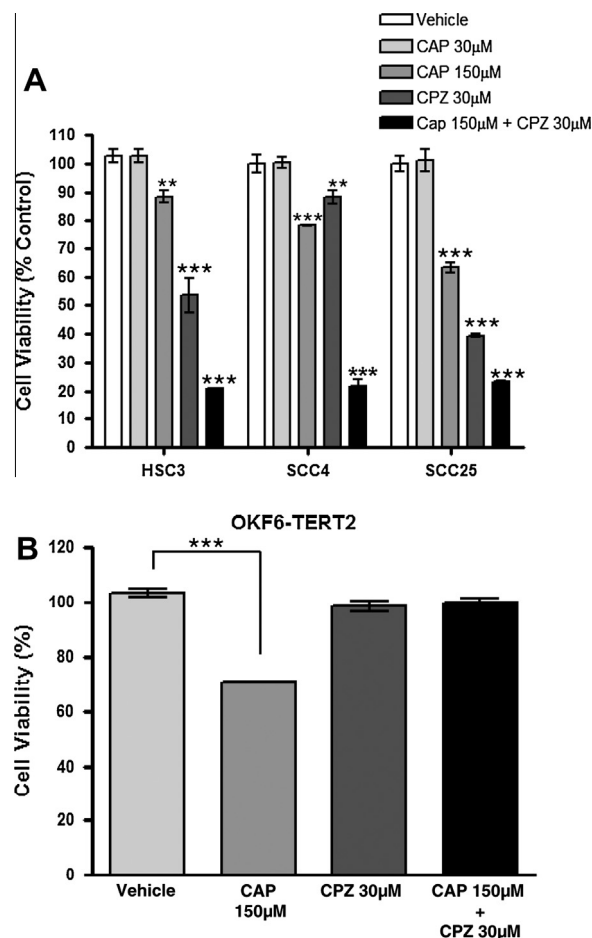

Figure 2. Cell viability assays reported as % vehicle control (n = 3). Panel A: OSCC cell lines treated with capsaicin (CAP) and/or capsazepine (CPZ) for 24 h compared to vehicle control. Panel B: immortalized oral keratinocytes OKF6-Tert2 cells treated with CAP and/or CPZ for 24 h compared to vehicle control; **p < 0.01, ***p < 0.001.
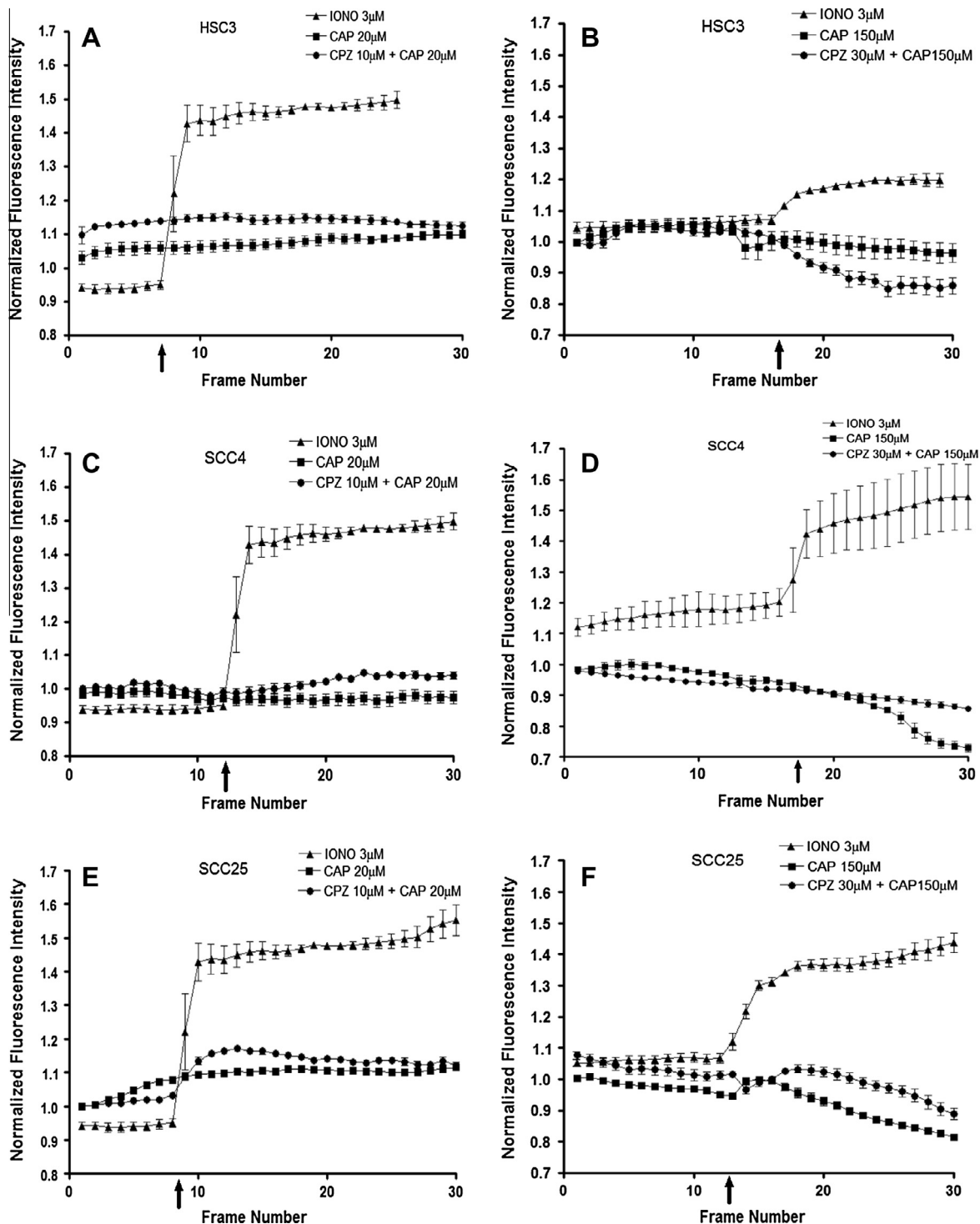
Figure 3. Calcium imaging of OSCC cell lines. *Panels A, C, and E:* OSCC cells treated with 20 μM CAP alone or in combination with 10 μM CPZ or treated with 3 μM ionomycin positive control ($n = 3$). *Panels B, D, and F:* OSCC cells treated with 150 μM CAP alone or in combination with 30 μM CPZ or treated with 3 μM ionomycin positive control ($n = 3$). Arrow indicates time point when treatment was added.

that TRPV1 is not functional under these conditions (Fig. 3A, C and E). Moreover no significant difference in TRPV1 channel activation was seen with capsaicin treatment alone or in combination with capsazepine. There was, however, a significant calcium influx ($p < 0.001$) in OSCC cells treated with the positive control, ionomycin (3 μM); a non-selective cation channel agonist. Treatment with cytotoxic concentrations (150 μM capsaicin and 30 μM capsazepine) also failed to induce calcium influx rather a slow release of

calcium was demonstrated following treatment with capsaicin alone or in combination with capsazepine (Fig. 3B, D and F).

Capsazepine induces apoptosis in OSCC cell lines

Based upon these findings, we evaluated the mechanism-of-action of capsazepine *in vitro*. It is hypothesized that vanilloids are analogues of Co-Q enzyme that effectively block electron

transport thereby generating ROS and inducing subsequent apoptosis [35]. To test this hypothesis, capsazepine treated cells were evaluated for ROS induction by DCF-DA staining and FACS analysis. All OSCC cell lines demonstrated an increase in ROS from their basal levels (Fig. 4A; solid line) that was reversed 92% in HSC3 cells, 65% in SCC4 cells and 59% in SCC25 cells when co-treated with NAC (10 mM) (Fig. 4B; solid line). Cell proliferation assays revealed that capsazepine (30 μM) cytotoxicity is also reversed ($p < 0.001$) by co-treatment with NAC (Fig. 5).

Microscopic analysis of OSCC cell lines treated with increasing concentrations of capsazepine (0 μM, 30 μM, 60 μM and 90 μM) for 24 h showed phenotypic changes characteristic of apoptosis including cell rounding and membrane blebbing (arrows) (Fig. 6). Higher capsazepine concentrations show large blebs and loss of plasma membrane integrity. Flow sort analysis revealed that capsazepine-treated cells had dose-dependent accumulation of cell populations in subG1 phase, consistent with apoptosis (Fig. 7A). Furthermore, western blot analysis showed increasing levels of
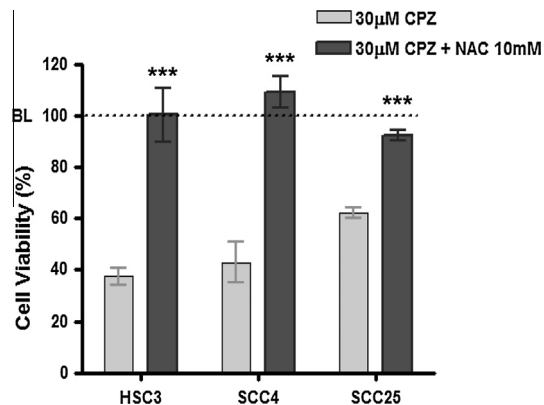

Figure 5. Cell viability assay of OSCC cell lines treated with 30 μM CPZ alone or in combination with 10 mM N-acetyl-cysteine (NAC) for 24 h ($n = 4$); ***$p < 0.001$.
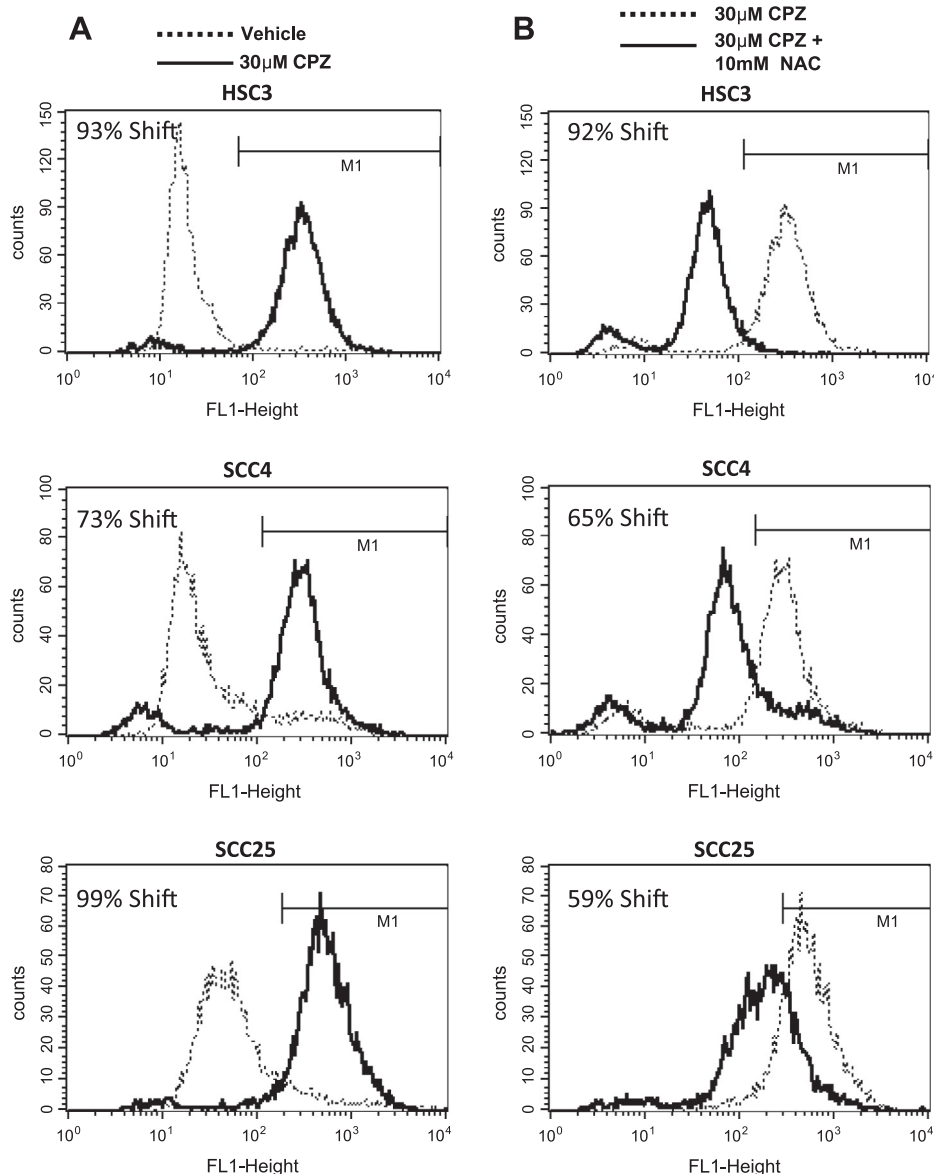

Figure 4. Induction of ROS in OSCC cell lines. *Panel A:* ROS induction in OSCC cell lines following 1 h treatment with 30 μM CPZ (black line) compared to vehicle control. *Panel B:* ROS induction in OSCC cell lines following 1 h treatment with 30 μM CPZ is reversed by NAC co-treatment (black line).
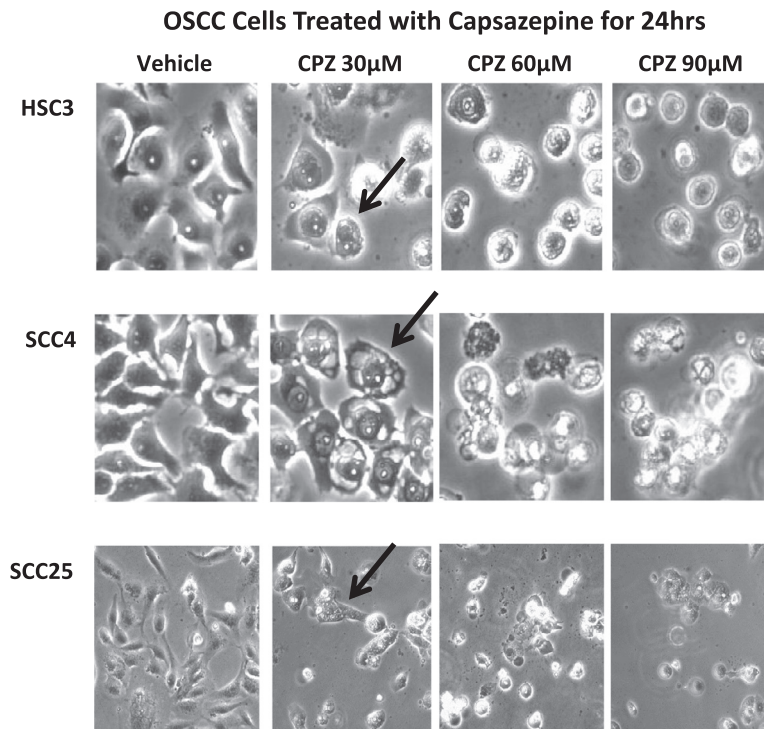
OSCC Cells Treated with Capsazepine for 24hrs

Figure 6. Capsazepine induced apoptosis in OSCC cell lines. Photomicrographs (10×) of OSCC cell lines treated with 0–90 µM CPZ for 24 h. Reduced confluency and increases in apoptotic figures are evident with increasing doses of CPZ (arrows).
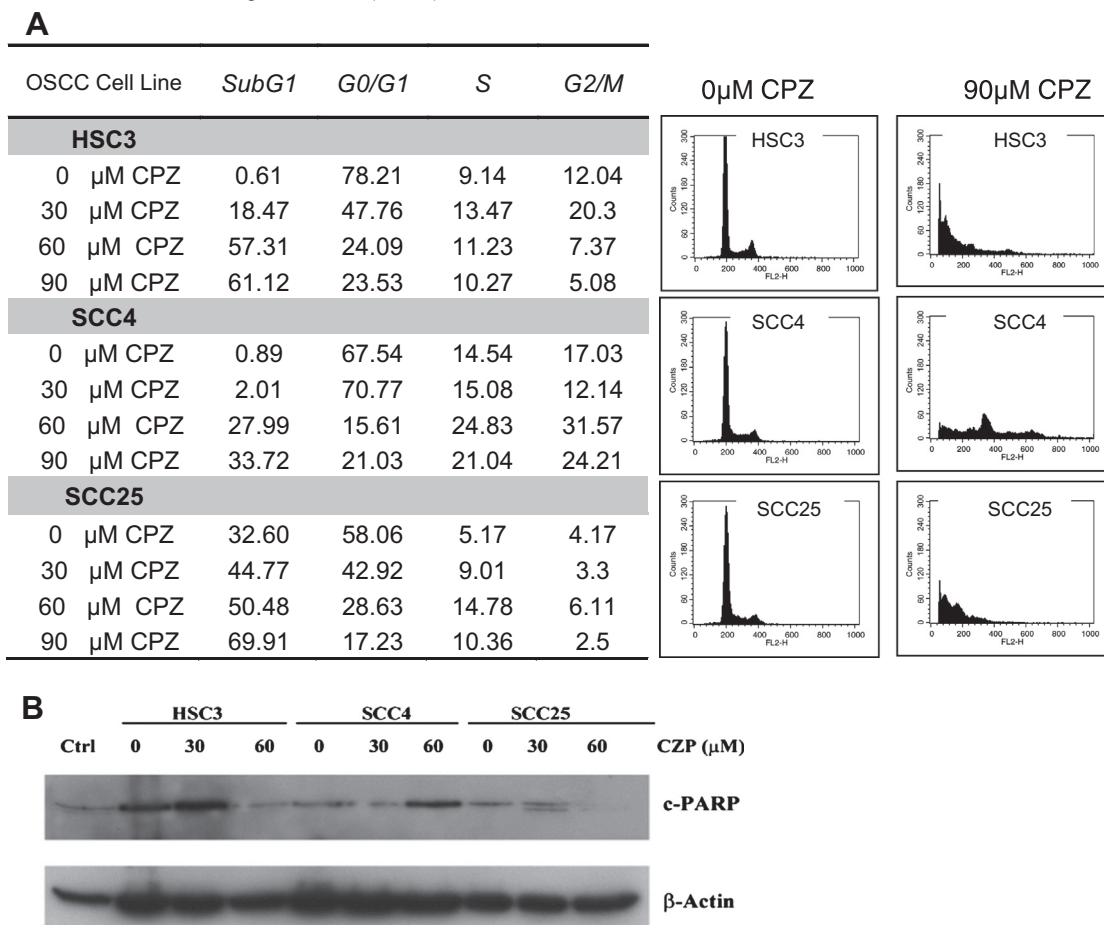
A

OSCC Cell Line	SubG1	G0/G1	S	G2/M
HSC3				
0 µM CPZ	0.61	78.21	9.14	12.04
30 µM CPZ	18.47	47.76	13.47	20.3
60 µM CPZ	57.31	24.09	11.23	7.37
90 µM CPZ	61.12	23.53	10.27	5.08
SCC4				
0 µM CPZ	0.89	67.54	14.54	17.03
30 µM CPZ	2.01	70.77	15.08	12.14
60 µM CPZ	27.99	15.61	24.83	31.57
90 µM CPZ	33.72	21.03	21.04	24.21
SCC25				
0 µM CPZ	32.60	58.06	5.17	4.17
30 µM CPZ	44.77	42.92	9.01	3.3
60 µM CPZ	50.48	28.63	14.78	6.11
90 µM CPZ	69.91	17.23	10.36	2.5

B

Figure 7. *Panel A*: Cell cycle distribution of OSCC cells (%) treated with 0–90 µM CPZ for 24 h with representative FACS for cells treated with 0 µM and 90 µM CPZ. All OSCC cell lines tested showed increased accumulation of cell population in subG1 phase that correlated with increasing doses of CPZ. *Panel B:* western blot analysis demonstrating induction of cleaved PARP (c-PARP) in OSCC cell lines treated with increasing doses of CPZ for 24 h; control is lysate from paclitaxel treated HeLa cells with known c-PARP activity.

cleaved PARP (c-PARP) in response to capsazepine treatments (Fig. 7B). Note that slower growing cells, HSC3 and SCC25, respond to capsazepine's cytotoxic effects at lower concentrations (30 μM) than fast-growing SCC4 cells, which require a higher capsazepine concentration (60 μM) to induce the apoptotic pathway (Fig. 7A and B). Consequently, a larger proportion of HSC3 and SCC25 cells become apoptotic when treated with 30 μM capsazepine and show greater induction of c-PARP compared to SCC4 cells at this concentration. Furthermore, 60 μM capsazepine treatments of HSC3 and SCC25 cells result in significant cell death and subsequent reduction in c-PARP. In contrast, SCC4 cells demonstrate a dose-dependent increase in c-PARP expression when treated with 30 μM and 60 μM capsazepine.

Capsazepine has anti-tumor effects in OSCC xenografts

SCC4 xenografts were fast-growing and non-invasive, SCC25 xenografts were slow-growing and invasive, and HSC3 xenografts were both fast-growing and invasive. Regardless of their unique characteristics, all OSCC xenograft models showed dramatic response to capsazepine resulting a significant reduction in tumor
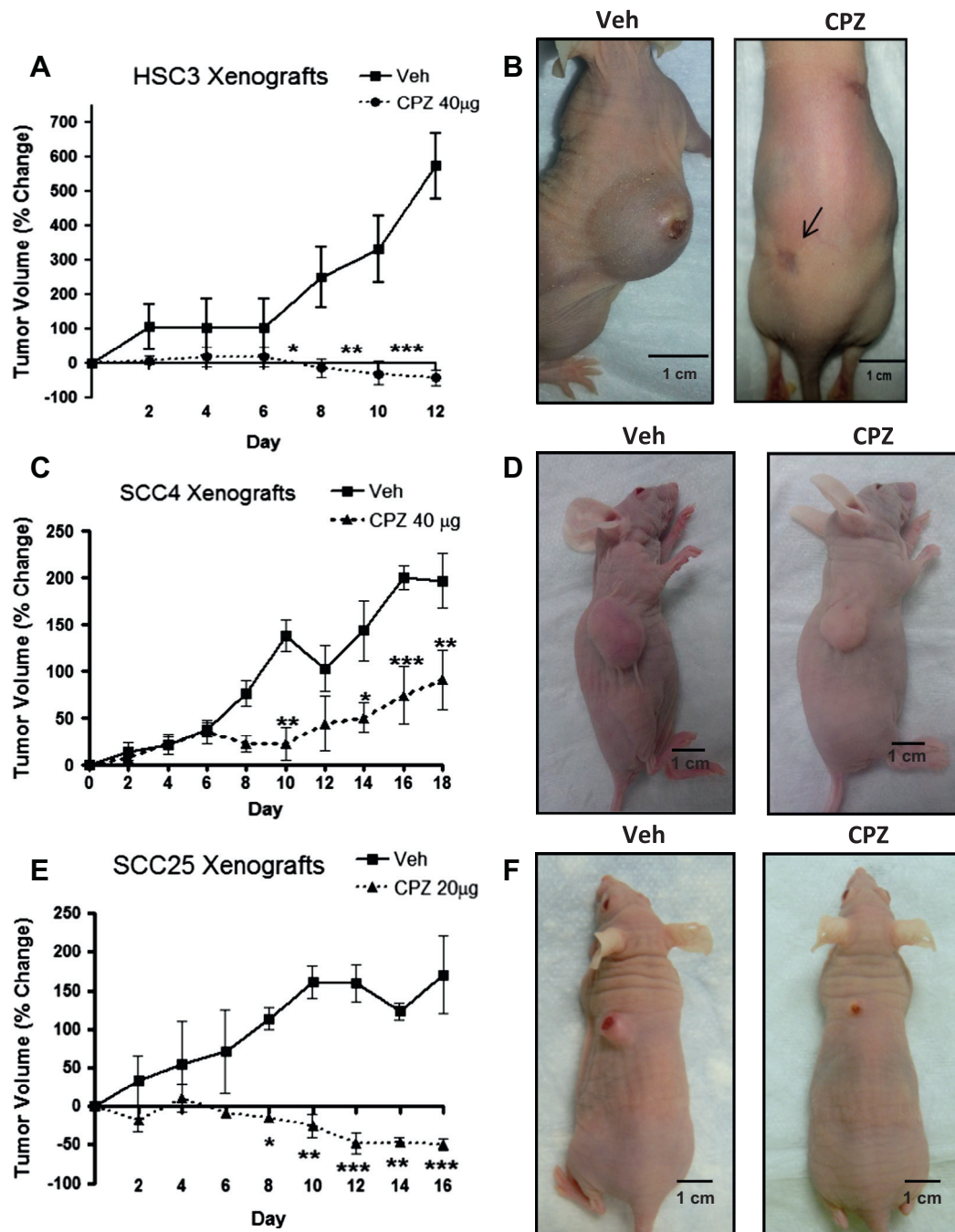

Figure 8. Anti-tumor effects of CPZ in OSCC xenograft models (n = 5). *Panel A:* HSC3 tumor growth (% change) when treated with 40 μg CPZ every other day for 12 days. *Panel B:* HSC3 xenograft treated with vehicle control (left panel) vs. 40 μg CPZ (right panel, arrow). *Panel C:* SCC4 tumor growth (% change) when treated with 40 μg CPZ every other day for 18 days. *Panel D:* SCC4 xenograft treated with vehicle control (left panel) vs. 40 μg CPZ (right panel). *Panel E:* SCC25 tumor growth (% change) when treated with 20 μg CPZ every other day for 16 days. *Panel F:* SCC25 xenograft treated with vehicle control (left panel) vs. 20 μg CPZ (right panel); $^*p < 0.05$, $^{**}p < 0.01$, $^{***}p < 0.001$.

volume (HSC3 & SCC25; $p < 0.05$) or a significant reduction in tumor growth rate (SCC4; $p < 0.05$) (Fig. 8).

HSC3 xenografts initially displayed a highly vascularized exophytic solid tumor mass. By day eight, control tumors grew significantly in size and were no longer a solid mass, rather they presented as a palpable fluid-filled mass (Fig. 8A and B left panel). Conversely, treated tumors did not enlarge and were not fluid filled

and, in fact, dramatically shrank in size (Fig. 8A and B). Healing looked complete in some tumor sites in HSC3 xenografts, with remaining scars indicative of the initial tumor that was present (Fig. 8B right panel; arrow). Upon sacrifice and dissection we confirmed that HSC3 xenografts were invasive fluid-filled tumors that contained a large amount of tumor cells. The dramatic difference in tumor volumes following twelve days of treatment is illustrated (Fig. 8A and B left panel). TUNEL staining on treated tumors confirmed the presence of apoptotic figures (Fig. 9A; arrow) however due to the invasive nature of untreated HSC3 tumors and the large amount of fluid, FFPE specimens could not be prepared for TUNEL analysis and quantification of apoptotic figures in HSC3 vehicle controls.

SCC4 xenografts were fast-growing solid exophytic tumors that failed to invade locally. By day ten, significant changes in tumor were seen and by the conclusion of the experiment control tumors grew nearly twofold greater than capsazepine treated tumors ($p < 0.01$; Fig. 8C and D). Histological analysis of H&E staining revealed a large necrotic core with viable tumor cells on the outer tumor margin. Therefore TUNEL staining was performed and apoptotic figures were quantified within the growing tumor front. We found significant increases in apoptotic figures in treated tumors ($p < 0.001$; Fig. 9B), which positively corresponds with our cell culture studies.

SCC25 xenografts were slow-growing exophytic solid tumors that failed to invade regional structures. These xenografts displayed a dramatic reduction in tumor volume following capsazepine treatments (50.5%, $p < 0.01$), in contrast control xenografts grew 170% during the experimental period (Fig. 8E and F). Histological analysis and TUNEL staining followed by quantification of apoptotic figures within the growing tumor front confirmed treated tumors had a significant increase in TUNEL staining ($p < 0.01$; Fig. 9C) reflecting the induction of apoptosis by capsazepine treatment that is also seen *in vitro*.

No negative effects on liver and kidney function were detected (Table 1). Furthermore, there were no adverse effects on healthy surrounding tissues and no detectable toxicities at the time of treatment. In accordance with the literature, animals displayed no changes in body temperature in response to treatment [36,37].
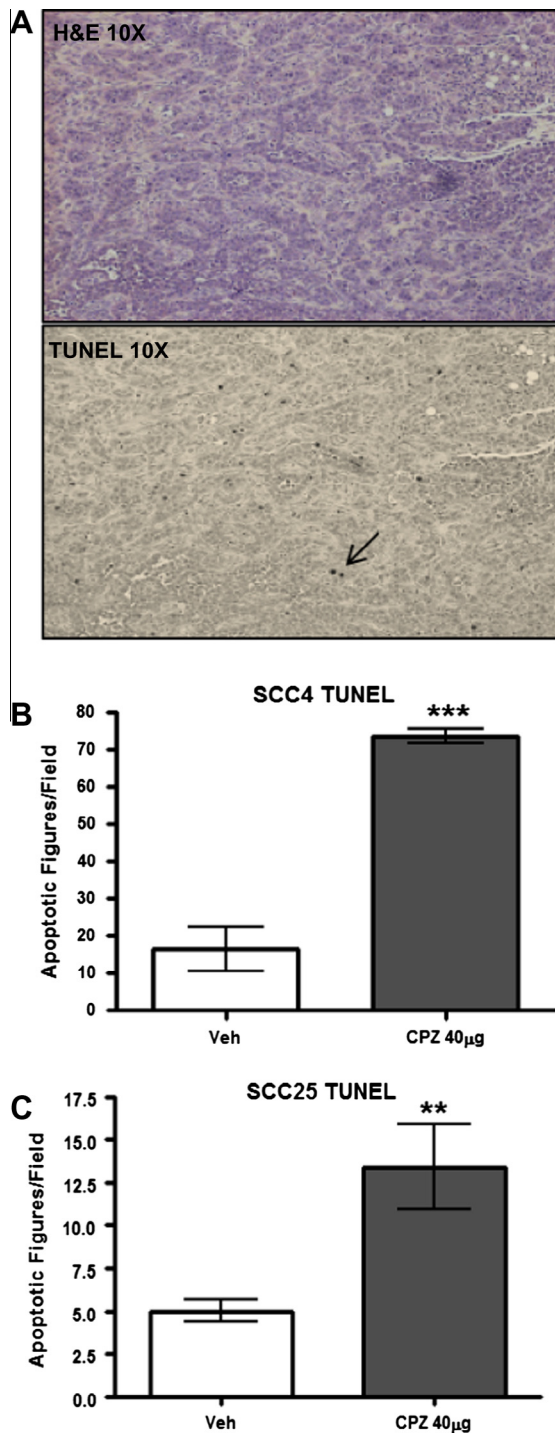
Discussion

Capsaicin was previously shown to induce apoptosis in mouse fibrosarcoma CSM5 cells, immortalized human bronchiolar epithelial cells, human lung adenocarcinoma cells (A549) and human hepatoma cells (HepG2), which underwent apoptosis when treated, *in vitro*, with the TRPV1 agonist, capsaicin [26,27]. Consistent with our findings, pre-treatment with capsazepine failed to inhibit capsaicin induced cytotoxicity even in TRPV1 over-expressing cells. In fact, capsazepine appeared to be more effective at inducing cell death than capsaicin [26,27]. This study confirms that vanilloids are cytotoxic to OSCC independent of TRPV1 activation.

In addition to functioning as a selective TRPV1 agonist, capsaicin is also an inhibitory quinone analogue that inhibits the plasma membrane-bound population of NADH oxidase in transformed cells [33–35]. Based on structural similarities, we hypothesize that the synthetic competitive TRPV1 antagonist, capsazepine, may also function by this mechanism. Indeed we show that treatment with capsazepine results in increased ROS, above basal levels, and induction of apoptosis that is reversed by NAC thereby suggesting that capsazepine may modulate cellular oxidative stress in OSCC. It is well documented that cancer cells are under oxidative stress due to their increased metabolic activity resulting in a delicate balance between ROS levels and the anti-oxidant capabilities of the cell [38,39]. Therefore increases in ROS, above basal level, disrupt this

Figure 9. TUNEL staining of OSCC xenografts. *Panel A:* representative photomicrograph of TUNEL stain of HSC3 xenograft (10X) treated with vehicle control. Arrow demonstrates apoptotic figure. *Panel B:* number of apoptotic figures per field in vehicle and CPZ (40 µg) treated SCC4 xenografts. *Panel C:* number of apoptotic figures per field in vehicle and CPZ (20 µg) treated SCC25 xenografts. Student's *t*-test of the average of six fields with $n = 3$; ***$p < 0.001$.

Table 1
Liver and kidney function tests for tumor bearing mice following treatment with vehicle control or CPZ.

Treatment	AST IU/L (r.v. = 107.4 ± 41.9)	ALT IU/L (r.v. = 24.8 ± 10.1)	CREA MG/DL (r.v. = 0.2 ± 0.1)	BUN MG/DL (r.v. = 17.1 ± 3.7)	Liver/body weight (g/100 g)	Kidney/body weight (g/100 g)
Control	137.4 ± 59.38	47.59 ± 15.68	0.0766 ± 0.008	24.52 ± 3.289	4.583 ± 0.553	1.470 ± 0.075
CPZ	101.3 ± 35.95	35.14 ± 8.013	0.0798 ± 0.015	21.98 ± 3.798	4.787 ± 0.017	1.315 ± 0.065

fine balance thereby triggering ROS induced apoptosis. This may explain why greater concentrations of capsazepine were required to inhibit fast-growing SCC4 cells.

Early studies evaluating capsaicin cytotoxicity in liver, ovarian, and breast cancer demonstrate that capsaicin cytotoxicity is limited to malignant cells with no adverse effects on non-malignant liver, ovarian, and breast cells *in vitro* [33,34]. However PC-3 prostate cancer xenografts treated locally with capsaicin resulted in pain and ulceration at the injection site [40]. Our study demonstrates that capsazepine is more effective at inhibiting cell viability than capsaicin at equal concentrations and the anti-tumor activity of capsazepine has no adverse effects on non-malignant tissues *in vitro and in vivo*.

Clinical trials assessing TRPV1 antagonists for the treatment of pain were discontinued due to severe hyperthermia that results from systemic administration of these drugs [41]. Like capsazepine, TRPV1 antagonists that block activation by capsaicin but fail to block activation by protons, such as AMG8562 and AMG7905, also do not induce hyperthermia in rats [36]. While AMG8562 fails to inhibit proton activation of TRPV1 in rats, it does inhibit all modes of TRPV1 activation in humans and therefore is predicted to induce hyperthermia in clinical trials [36,37]. Our study confirms that capsazepine does not induce hyperthermia in a rodent model however it is yet to be tested in clinical trials. Should capsazepine prove to induce hyperthermia in humans, then this study demonstrates the potential for local injection to circumvent hyperthermia while maintaining significant anti-tumor effects. This may prove useful both in palliative care and in prolonging life for OSCC patients.

In summary, these novel findings demonstrate that local delivery of capsazepine effectively slows, reverses, and even terminates OSCC tumor growth without the potential adverse effects of capsaicin. Our data also suggest that capsazepine actions may be mediated by inducing ROS and apoptosis in OSCC. Capsazepine may therefore prove to be an efficacious, novel approach to treat OSCC.

Conflict of interest statement

The University of Texas Health Science Center at San Antonio has claimed intellectual property on findings reported in this study.

Acknowledgments

References

[1] Cancer Facts and Figures 2012. Atlanta: American Cancer Society; 2012.
[2] Henry MA, Hargreaves KM. Peripheral mechanisms of odontogenic pain. Dent Clin North Am 2007;51:19–44 (v.).
[3] Caterina MJ, Schumacher MA, Tominaga M, Rosen TA, Levine JD, Julius D. The capsaicin receptor: a heat-activated ion channel in the pain pathway. Nature 1997;389:816–24.
[4] Nilius B, Talavera K, Owsianik G, Prenen J, Droogmans G, Voets T. Gating of TRP channels: a voltage connection? J Physiol 2005;567:35–44.
[5] Prevarskaya N, Zhang L, Barritt G. TRP channels in cancer. Biochim Biophys Acta 2007;1772:937–46.
[6] Deeds J, Cronin F, Duncan LM. Patterns of melastatin mRNA expression in melanocytic tumors. Hum Pathol 2000;31:1346–56.
[7] Duncan LM, Deeds J, Cronin FE, Donovan M, Sober AJ, Kauffman M, et al. Melastatin expression and prognosis in cutaneous malignant melanoma. J Clin Oncol 2001;19:568–76.
[8] Duncan LM, Deeds J, Hunter J, Shao J, Holmgren LM, Woolf EA, et al. Down-regulation of the novel gene melastatin correlates with potential for melanoma metastasis. Cancer Res 1998;58:1515–20.
[9] Fang D, Setaluri V. Expression and Up-regulation of alternatively spliced transcripts of melastatin, a melanoma metastasis-related gene, in human melanoma cells. Biochem Biophys Res Commun 2000;279:53–61.
[10] Fuessel S, Sickert D, Meye A, Klenk U, Schmidt U, Schmitz M, et al. Multiple tumor marker analyses (PSA, hK2, PSCA, trp-p8) in primary prostate cancers using quantitative RT-PCR. Int J Oncol 2003;23:221–8.
[11] Mergler S, Strowski MZ, Kaiser S, Plath T, Giesecke Y, Neumann M, et al. Transient receptor potential channel TRPM8 agonists stimulate calcium influx and neurotensin secretion in neuroendocrine tumor cells. Neuroendocrinology 2007;85:81–92.
[12] Tsavaler L, Shapero MH, Morkowski S, Laus R. Trp-p8, a novel prostate-specific gene, is up-regulated in prostate cancer and other malignancies and shares high homology with transient receptor potential calcium channel proteins. Cancer Res 2001;61:3760–9.
[13] Prevarskaya N, Skryma R, Bidaux G, Flourakis M, Shuba Y. Ion channels in death and differentiation of prostate cancer cells. Cell Death Differ 2007;14:1295–304.
[14] Domotor A, Peidl Z, Vincze A, Hunyady B, Szolcsanyi J, Kereskay L, et al. Immunohistochemical distribution of vanilloid receptor, calcitonin-gene related peptide and substance P in gastrointestinal mucosa of patients with different gastrointestinal disorders. Inflammopharmacology 2005;13:161–77.
[15] Hartel M, di Mola FF, Selvaggi F, Mascetta G, Wente MN, Felix K, et al. Vanilloids in pancreatic cancer: potential for chemotherapy and pain management. Gut 2006;55:519–28.
[16] Lazzeri M, Vannucchi MG, Spinelli M, Bizzoco E, Beneforti P, Turini D, et al. Transient receptor potential vanilloid type 1 (TRPV1) expression changes from normal urothelium to transitional cell carcinoma of human bladder. Eur Urol 2005;48:691–8.
[17] Sanchez MG, Sanchez AM, Collado B, Malagarie-Cazenave S, Olea N, Carmena MJ, et al. Expression of the transient receptor potential vanilloid 1 (TRPV1) in LNCaP and PC-3 prostate cancer cells and in human prostate tissue. Eur J Pharmacol 2005;515:20–7.
[18] Fixemer T, Wissenbach U, Flockerzi V, Bonkhoff H. Expression of the Ca2+-selective cation channel TRPV6 in human prostate cancer: a novel prognostic marker for tumor progression. Oncogene 2003;22:7858–61.
[19] Peng JB, Chen XZ, Berger UV, Weremowicz S, Morton CC, Vassilev PM, et al. Human calcium transport protein CaT1. Biochem Biophys Res Commun 2000;278:326–32.
[20] Peng JB, Zhuang L, Berger UV, Adam RM, Williams BJ, Brown EM, et al. CaT1 expression correlates with tumor grade in prostate cancer. Biochem Biophys Res Commun 2001;282:729–34.
[21] Wissenbach U, Niemeyer B, Himmerkus N, Fixemer T, Bonkhoff H, Flockerzi V. TRPV6 and prostate cancer: cancer growth beyond the prostate correlates with increased TRPV6 Ca2+ channel expression. Biochem Biophys Res Commun 2004;322:1359–63.
[22] Zhuang L, Peng JB, Tou L, Takanaga H, Adam RM, Hediger MA, et al. Calcium-selective ion channel, CaT1, is apically localized in gastrointestinal tract epithelia and is aberrantly expressed in human malignancies. Lab Invest 2002;82:1755–64.
[23] Clapham DE, Julius D, Montell C, Schultz G. International Union of Pharmacology. XLIX. Nomenclature and structure-function relationships of transient receptor potential channels. Pharmacol Rev 2005;57:427–50.
[24] Tomohiro D, Mizuta K, Fujita T, Nishikubo Y, Kumamoto E. Inhibition by capsaicin and its related vanilloids of compound action potentials in frog sciatic nerves. Life Sci 92:368–378.
[25] Bevan S, Hothi S, Hughes G, James IF, Rang HP, Shah K, et al. Capsazepine: a competitive antagonist of the sensory neurone excitant capsaicin. Br J Pharmacol 1992;107:544–52.
[26] Ghosh AK, Basu S. Fas-associated factor 1 is a negative regulator in capsaicin induced cancer cell apoptosis. Cancer Lett 287:142–149.
[27] Reilly CA, Taylor JL, Lanza DL, Carr BA, Crouch DJ, Yost GS. Capsaicinoids cause inflammation and epithelial cell death through activation of vanilloid receptors. Toxicol Sci 2003;73:170–81.

[28] Saghafi N, Lam DK, Schmidt BL. Cannabinoids attenuate cancer pain and proliferation in a mouse model. Neurosci Lett 488:247–251.

[29] Livak KJ, Schmittgen TD. Analysis of relative gene expression data using real-time quantitative PCR and the 2(-Delta Delta C(T)) Method. Methods 2001;25:402–8.

[30] Jeske NA, Por ED, Belugin S, Chaudhury S, Berg KA, Akopian AN, Henry MA, Gomez R. A-kinase anchoring protein 150 mediates transient receptor potential family V type 1 sensitivity to phosphatidylinositol-4,5-bisphosphate. J Neurosci 31:8681–8688.

[31] Tinley TL, Leal RM, Randall-Hlubek DA, Cessac JW, Wilkens LR, Rao PN, et al. Novel 2-methoxyestradiol analogues with antitumor activity. Cancer Res 2003;63:1538–49.

[32] Jensen MM, Jorgensen JT, Binderup T, Kjaer A. Tumor volume in subcutaneous mouse xenografts measured by microCT is more accurate and reproducible than determined by 18F-FDG-microPET or external caliper. BMC Med Imaging 2008;8:16.

[33] Kim S, Moon A. Capsaicin-induced apoptosis of H-ras-transformed human breast epithelial cells is Rac-dependent via ROS generation. Arch Pharm Res 2004;27:845–9.

[34] Morre DJ, Chueh PJ, Morre DM. Capsaicin inhibits preferentially the NADH oxidase and growth of transformed cells in culture. Proc Natl Acad Sci USA 1995;92:1831–5.

[35] Ziglioli F, Frattini A, Maestroni U, Dinale F, Ciufifeda M, Cortellini P. Vanilloid-mediated apoptosis in prostate cancer cells through a TRPV-1 dependent and a TRPV-1-independent mechanism. Acta Biomed 2009;80:13–20.

[36] Ayoub SS, Hunter JC, Simmons DL. Answering the burning question of how transient receptor potential vanilloid-1 channel antagonists cause unwanted hyperthermia. Pharmacol Rev 2009;61:225–7.

[37] Lehto SG, Tamir R, Deng H, Klionsky L, Kuang R, Le A, Lee D, Louis JC, Magal E, Manning BH, et al. Antihyperalgesic effects of (R,E)-N-(2-hydroxy-2,3-dihydro-1H-inden-4-yl)-3-(2-(piperidin-1-yl)-4-(trifluorom ethyl)phenyl)-acrylamide (AMG8562), a novel transient receptor potential vanilloid type 1 modulator that does not cause hyperthermia in rats. J Pharmacol Exp Ther 2008;326:218–29.

[38] Pelicano H, Carney D, Huang P. ROS stress in cancer cells and therapeutic implications. Drug Resist Updat 2004;7:97–110.

[39] Konstantinov AA, Peskin AV, Popova E, Khomutov GB, Ruuge EK. Superoxide generation by the respiratory chain of tumor mitochondria. Biochim Biophys Acta 1987;894:1–10.

[40] Sanchez AM, Sanchez MG, Malagarie-Cazenave S, Olea N, Diaz-Laviada I. Induction of apoptosis in prostate tumor PC-3 cells and inhibition of xenograft prostate tumor growth by the vanilloid capsaicin. Apoptosis 2006;11:89–99.

[41] Brederson JD, Kym PR, Szallasi A. Targeting TRP channels for pain relief. Eur J Pharmacol.